World Academy of Science, Engineering and Technology
International Journal of Physical and Mathematical Sciences
Vol:5, No:11, 2011

Numerical Study on Parametrical Design of Long Shrouded Contra-Rotating Propulsion System in Hovering

Chao. Huo, Roger. Barènes, Jérémie. Gressier and Gilles.Grondin

***Abstract*—**The parametrical study of Shrouded Contra-rotating Rotor was done in this paper based on 2D axisymmetric simulations. The calculations were made with an actuator disk as double rotor model. It objects to explore and quantify the effects of different shroud geometry parameters mainly using the performance of power loading (PL), which could evaluate the whole propulsion system capability as 5 Newtontotal thrust generationfor hover demand. The numerical results show that:The increase of nozzle radius is desired but limited by the flow separation, its optimal design is around 1.15 times rotor radius, the viscosity effects greatly constraint the influence of nozzle shape, the divergent angle around 10.5° performs best for chosen nozzle length;The parameters of inlet such as leading edge curvature, radius and internal shape do not affect thrust great but play an important role in pressure distribution which could produce most part of shroud thrust, they should be chosen according to the reduction of adverse pressure gradients to reduce the risk of boundary separation.

***Keywords*—**Axisymmetric simulation, parametrical design, power loading, Shrouded Contra-Rotating Rotor.

I. Introduction

THE shrouded rotor(s) configuration has emerged as the most popular choice for rotary-wing Micro Air vehicles (MAVs), because of the inherent safety and potential for significant performance improvements such as propulsion efficiency and static thrust, along with noise reduction due to the presence of shroud [1]-[2]. In views of these advantages, many companies have applied this conception on several MAVs such as Sikorsky's Cypher, Allied Aerospace's iSTAR and so on [3]-[5].

However, generally for these MAVs the shroud is restricted in size to a dimension of about 15cm. It induces a very low Reynolds number (< 20,000)flows inside the shroud and on the rotor blades. The traditional duct design philosophies based on experience with large-scale ducted propellers thus may not be applied to it. Until now, some efforts have been made in governments, industries and academic communities to aim at design issues for this class of propulsion system, and it has been developed to investigate the shroud shape optimization. A few of parametric studies were done by Black, Wainauski, Jason and so on [1], [6]-[7].They identified the shroud exit area ratio is one of most important design parameters in the shrouded rotor systems. But experimental studies on the shrouded rotors system for exploring the shroud effects have relied mostly on wind tunnel experiments, and for the shroud design issues such as parametrical studies have been limited to a few due to the cost of different shroud models and the complication of the experimental methods. Then the simulation seems to be a very important tool to offer some basic design criteria. However the current studies havemostly focused on the whole vehicles' modeling, aerodynamic design, control, stability and so on[8]-[12].

Therefore this paper focuses on parametrical study of shroud in hovering based on 2D axisymmetricsimulation methods, which can show a design direction, as well as on the contribution to more physical understanding of the shrouded contra-rotating rotor system. Since this paper targets to design the shroud in order to make the whole propulsion system consume less mechanical power with a constant thrust generation of 5 Newton which balances the overall weight of the whole vehicle, the double rotor will be modeled as an actuator disk according to the Froude theory in order to simplify the cases and reduce the computation cost. The parameters of different shroud components—inlet, cylindrical section and nozzle will be analyzed one by one.

II. Analytical Model

The shrouded contra-rotating rotor is composed of two parts: the double rotor and the shroud. The two rotors rotate at the opposite direction and are installed inside the shroud at the same axis showed in the Fig.1(a). The overall configuration is axisymmetric. The analytical models for each part will be explained in detail as following sections.

A. Rotor modeling with actuator disk

As a resource to transform the mechanical power to kinetic energy, the double rotor is obviously a key part for the rotary vehicles. Since this work emphasizes on the shroud parameters design, the main effect of rotor(s') could be replaced by an actuator diskfor the shrouded rotating propulsion systems. It simplifies the rotor(s) as a flat and infinitely thin disk which

C. Huoiswith the Institut Supérieur de l'Aéronautique et de l'Espace, 10 av. Edouard Belin – BP 54032 31055, Toulouse, France (phone: 33-0561338926; fax: 33-0562178347; e-mail: huochao1023@ Hotmail.com, c.huo@isae.fr).

R. Barènes is with the Institut Supérieur de l'Aéronautique et de l'Espace, 10 av. Edouard Belin – BP 54032 31055, Toulouse, France (e-mail: roger.barenes@isae.fr).

J. Gressier is with the Institut Supérieur de l'Aéronautique et de l'Espace, 10 av. Edouard Belin – BP 54032 31055, Toulouse, France (e-mail: jeremie.gressier@isae.fr).

G. Grondin is with the Institut Supérieur de l'Aéronautique et de l'Espace, 10 av. Edouard Belin – BP 54032 31055, Toulouse, France (e-mail: gilles.grondin@isae.fr).

produces a uniform pressure jump between both sides of the disc. The general configuration of the model is modified as showed in the Fig. 1(b).

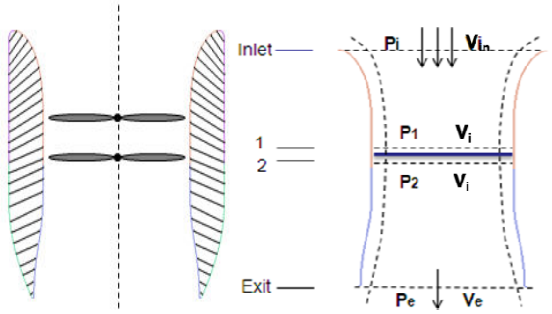

a. System configuration scheme b. Froude model for shrouded system
Fig.1 Shrouded contra-rotating rotor configuration and Froude model

Compared with free rotating systems, the behavior of the air fluid is cowled by the shroud which is featured in particular with two new geometrical parameters:

$$K_i = \frac{A_i}{A_R}; K_e = \frac{A_e}{A_R} \quad (1)$$

Where A_i , A_R,A_e denote the inlet, rotor and nozzle exit area respectively. For the inlet area, it is defined as the zone on which the mass flow comes inside the system. So it exists the regime: $\pi {R_{le}}^2 < A_i < \infty$. Here R_{le} is the leading edge radius on the shroud geometry which will be introduced in detail as following sections.

Combined with the Froude theory which applies the Bernoulli equation, momentum equation and mass conservation, it could easily explore how the flow is developed from far upstream to far downstream on this propulsion system with the rotor(s) modeled as an actuator disk. The far upstream velocity is generally considered as zero according to the environment condition. And the global performances of the shrouded rotor(s) system can be evaluated as following equations:

Total thrust:

$$\frac{F_T}{\rho \cdot A_R} = \left(\frac{1}{K_e} - \frac{1}{2K_i}\right) \cdot \left(\frac{\dot{m}}{\rho \cdot A_R}\right)^2 \quad (2)$$

Rotor thrust:

$$\frac{F_R}{\rho \cdot A_R} = \frac{1}{2} \cdot \frac{1}{{K_e}^2} \cdot \left(\frac{\dot{m}}{\rho \cdot A_R}\right)^2 \quad (3)$$

The thrust of inlet:

$$\frac{F_{in}}{\rho \cdot A_R} = \frac{1}{2}\left(\frac{K_i - 1}{K_i}\right) \cdot \left(\frac{\dot{m}}{\rho \cdot A_R}\right)^2 \quad (4)$$

The thrust of nozzle:

$$\frac{F_{noz}}{\rho \cdot A_R} = \frac{1}{2}\left(-\left(\frac{K_e - 1}{K_e}\right)^2\right) \cdot \left(\frac{\dot{m}}{\rho \cdot A_R}\right)^2 \quad (5)$$

Here, the induced velocity of flow on the rotor is:

$$V_i = \frac{\dot{m}}{\rho \cdot A_R} \quad (6)$$

From the model configuration showed above, in the 2D numeric simulation, the thrust generated by rotor can be also calculated in the following equations.

$$F_R = \Delta P \cdot A_R = (P_2 - P_1) \cdot A_R \quad (7)$$

Under the condition of nozzle adaptation, by introducing (3) into (7), ΔP could be calculated:

$$\Delta P = \frac{1}{2} \cdot \frac{1}{{K_e}^2} \cdot \left(\frac{\dot{m}}{\rho \cdot A_R}\right)^2 \cdot \rho \quad (8)$$

For the mass flow, the thrust of different components, the power which will be introduced as following sections etc., the dependencies on ΔP could be obtained according to this expression.

From the equations above, the kinetic energy from the mechanical power contribute to different components of the shrouded system in the form of the coefficients with the two geometry parameters $K_i$and K_e. This theoretical method for calculating aerodynamic parameters for a shrouded system is definitely limited. Although K_i is considered in the Froude theory, but its effect is uncertain compared to K_e . That is quite hard to obtain its specific effect and also the effectsfrom otherdifferent parameters. What the most important is that the flow is one dimensional and it assumes the flow is uniform on the radial direction of the system, which is not realistic and significantly affects the calculation accuracy. In view of the advantage of higher efficient and lower cost, the 2D simulation with the rotor modeled by an actuator disk is obviously a wayto specify the designs of each parameter.

B. Shroud models and the extraction of geometric parameters

Basically, the main idea of shroud cross-section profile comes from the geometry of airfoil because of the aerodynamic principles to produce the lift. For the shrouded system, the purpose for applying shroud is to generate the thrust. This drives the shroud design method distinguish with the airfoil. According to the functions of different shroud parts, the shroud could be separated into three parts: inlet, middle cylindrical section and nozzle.

For the shroud inlet, its importance is that the incoming air forms a low pressure region on the inlet lip, which is the main reason why the shroud generates thrustitself. Under the hovering situation, the rotating rotor with the shroud aspirates the air from all around the propulsion system, a suction peak is therefore formed on the inlet; For the cylindrical section in the middle, it offers a space to double rotor which has to minimize the gap between the shroud and rotor tip to reduce the tip vortex loss; The nozzle function is to expand the slipstream after the rotor. This could decrease the final wake velocity and increase the mass flow through the rotor.

For each part, as the way to constraint the shroud profile, all of the possible geometrical parameters are extracted as Fig.2.In

the figure, the parameters considered include: length l_i , internal shape, leading edge curvature C_{le} and leading edge radius R_{le} for the inlet; maximum radius R_{max} and cylindrical radius for the whole system and specially for the cylindrical section; exit radius R_e , length $l_N$and internal shape for the nozzle. Here the cylindrical radius is the rotor radius R_{rot} once the Froude theory or actuator disk is applied in the simulation.

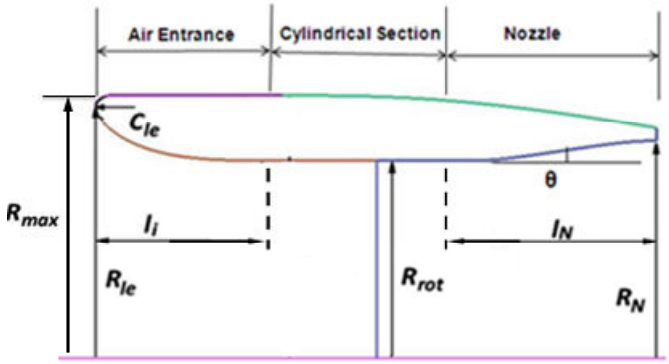

Fig. 2 Geometrical parameters of shroud

In this paper, the rotor radius will be fixed to 90 mm. The computational different shroud models will be given with one changeable geometry parameters and others keeping constant to explore their effects independently.

III. Numerical Methodology

During 2D axisymmetric simulation, the Finite Volume Method (FVM) was used to discretethe basic governing equations from the conservation laws of fluid mechanics.

For this propulsion system at the normal operational condition, because its Mach number is generally far smaller than 0.3 and the Reynolds number is much greater than 3000, the aerodynamic flow could be considered incompressible and turbulent. In order to solve the turbulent flow, the Reynolds Average Navier-Stokes equations and Spalart-Allmaras model were chosen in this work.

A. Computational field and boundary condition

As the explanation for the geometry, the shrouded system was simplified as a 2D axisymmetric configuration, hence the necessary computed field was half of the structure. Meanwhile in order to avoid the definition of the boundary condition in inlet and outlet surface of shroud because of the uniform radial pressure gradient, and also to obtain the flow information as much as possible, the computational field did not only include the shroud internal flow filed but also contain a huge zone around the shroud. The axisymmetric computational field is shown in Fig.3. The computed field is composed by the air inlet and outlet, the shrouded system with an actuator disk, and the symmetric axis.

The boundary definition corresponding to the geometry could be seen in the Fig.3. For the shrouded system, the rotor was modeled as an actuator disk which was defined as fan boundary producing the pressure discontinuity in the flow properties. Flow was imposed slowly on the inlet and outlet, and also when the calculation is initialed in order to keep from the reversed flow at the outlet boundary, which could induce a nonphysical solution and also the convergence problem. The pressure condition was used at outlet that is quite close to the reality.

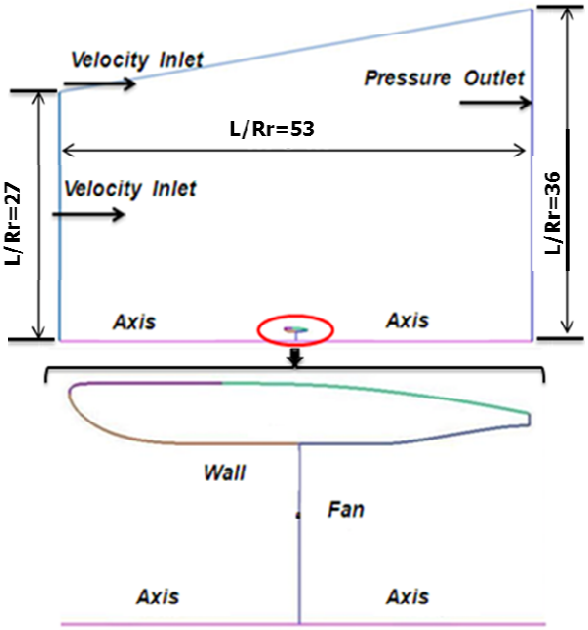

Fig. 3 Computational field and boundary condition settings

B. Axisymmetric mesh generation

Since the flow is considered turbulent and solved with Spalart-Allmaras turbulence model, which is a low-Reynolds number model in its complete implementation. This means it is used with the meshes properly resolving the viscous-affected region, and damping functions have been built into the model in order to properly attenuate the turbulent viscosity in its sublayer. Therefore, compared to the coarse mesh with $Y^+ \geq 30$ for standard wall function, to obtain the full benefit of the Spalart-Allmaras model, the mesh space of shroud near-wall should be lower than 1 for enhanced wall treatment.

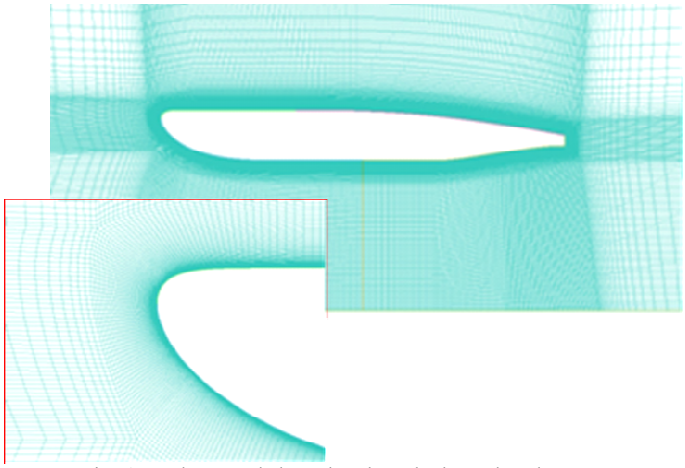

Fig. 4 Mesh around shroud and on the boundary layer

As showed in Fig.4, a structure hexahedral mesh that satisfies the condition of $Y^+ < 1$ was generated. The O-grid produced around the shroud gives the possibility to refine the mesh and have a better solution of the boundary layer.

C. Evaluation parameters

Generally, in order to evaluate the propulsion system, the propulsive efficiencyη showed in following equation is always adopted.

$$\eta = \frac{(F_{R1}+F_{R2}+F_S)\cdot V_0}{Q_1\cdot\omega_1+Q_2\cdot\omega_2} \quad (9)$$

Here F_{R_1}, F_{R_2} and F_s are the thrusts of first rotor, second rotor and shroud respectively, V_0 is the velocity of vehicle, $Q_i$andω_i mean the torque and angular velocity of each rotor.

The equation implies the system with a high efficiency could covert the available mechanical power into the kinetic energy for supporting the flight of whole propulsion system. However, the work in this paper focused on the hovering performance of the shrouded system. It means the system velocity keeps zero ($V_0 = 0$) when the vehicle hovers in the space. This propulsive efficiency cannot be used for the shrouded system in hovering. Another one usually applied is the Figure of Merit (FoM). It is used to qualify the ability of rotor to transform the mechanical power to the flow. As for the rotor in this paper, it was modeled as actuator disk and it is assumed that the rotor perfectly convert the mechanical power into the kinetic energy of the flow. This implies that these two variables which generally evaluate the rotorcraft propulsion system are not suitable for this 2D axisymmetric simulation.

Therefore another quantity -- power loading is proposed to evaluate the system. Its definition is:

$$PL = \frac{F_T}{W} \qquad [N/Watt] \quad (10)$$

Obviously, the optimal design should produce a maximum total thrust F_T but consume minimum power W. In 2D simulation, as talked above, the actuator disk is capable of energy conversion, so the power could be calculated with the pressure jump which is imposed on the actuator disk as a "fan boundary condition"in (11).

$$W = \frac{\Delta P\cdot\dot{m}}{\rho} \qquad [Watt] \quad (11)$$

IV. Results and Discussion

As mentioned in the introduction, the desired overall weight of whole vehicle is 5 Newton, the applied shrouded contra-rotating rotor aims to generate the same thrust to maintain the static condition or hovering. But it is difficult to evaluate the specific value of pressure jump imposed on the fan boundary condition that could achieve the global thrust generation of 5N. Therefore the simulation was conducted firstly at a pressure jump of 100 Pascal, then the second time was made to obtain the desired thrust 5N based on the calculation between total thrust and pressure jump as introduced in the equations (2)-(8) from last simulation. According to this way, with constant rotor diameter 90mm, the effects of shroud geometry parameters were analyzed.

A. Influence of nozzle design parameters

Nozzle is an important component for shroud, it is used to expand the flow after rotor and affect the absorbing mass flow. For the profile of nozzle showed in the Fig.2, it is defined by nozzle exit radius, length and the internal shape.

1). Nozzle exit radius

The nozzle exit radius was changed from $R_e = 80$ mmto $R_e = 115$ mm with the step of 5 mm which is correspondent to the ratio from 0.89 to 1.28of nozzle exit radius divided by rotor radius. Fig.5 shows the configurations of both extreme cases.

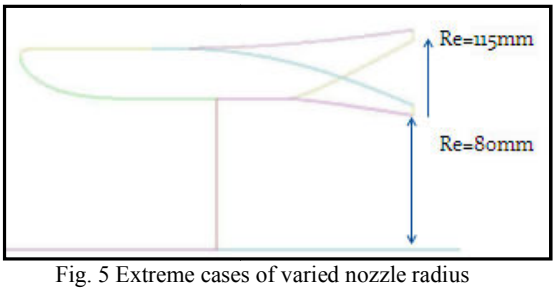

Fig. 5 Extreme cases of varied nozzle radius

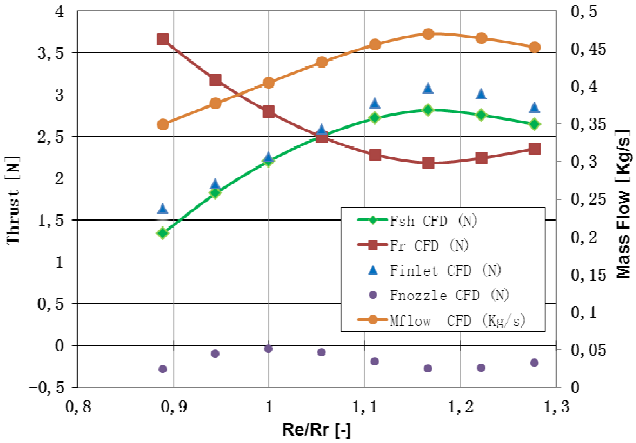

Fig. 6 Thrust of shroud and its components for given Ft of 5N

With changing nozzle exitradiusR_e, the contributions of different components from shroud are changed too as showed in Fig.6. For the demand to produce total thrust 5N, the mass flow $\dot{m}$is increased with the increment of R_e. This implies the relative greater nozzle radius can expand the flow better so that more air is absorbed inside the shrouded system. The shroud consequently produces more thrust (F_{sh}) and its contribution becomes more important until R_e equal to 1.15 times the rotor radius. At this value, the shroud could generate greater than 50% thrust of the total one.For such contribution, it mainly comes from the air entrance part (F_{inlet}). And the nozzle alwaysgenerates a negative thrust (F_{nozzle}). But this could not mean there is no sense to apply it. The basic reason of thrust production for shroud inlet and nozzle is the pressure distribution on their surfaces due to the mass flow $\dot{m}$. Meanwhile, since the shroud produces more and more thrust, it naturally makes the importance of the rotor (F_r) becomes less for a total thrust demand 5N.

However, after $R_e > 1.18R_r$, Fig.6 shows a condition on the contrary, the increased R_e leads to a decreased thrust performance with the decreased mass flow. Thelimited improvementis due to the flow separation seen in Fig.7. Fig.7

shows the velocity magnitude distribution around the shroud. The flow separation appears on the boundary layer of the nozzle with great radius ratio $R_e/R_r = 1.22$.

One effect of the flow separation is a loss of total pressure, and another is the thickeningof the boundary layer on the nozzle. This effect is to reduce the effective nozzle radius. Another physical phenomenon is the vortex on the up corner of shroud trailing edge. This might be more severe when exit nozzle radius R_e is increased greater than the radius of shroud cylindrical section.

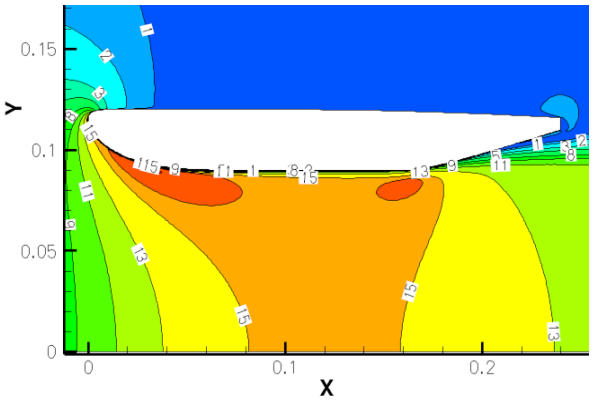

Fig. 7 Velocity magnitude distribution for $R_e/R_r = 1.22$

Besidesthe realization on the performance with increased R_e from the simulation, according to the introduction on the Froude theory in the section of analytical model, a comparison to the simulationon the shroud thrust was made in order to clear the behavior of the system. Fig.8 shows the shroud thrust from the Froude theory based on the equations (2)-(8) with $K_i = \infty$(infinite) and 1.63 respectively and the 2D axisymmetric simulation result as well.

In Fig.8, globally the tendencies of the shroud thrust with the increased nozzle radius are similar in both simulation and Froude theory. And the simulation result is more close to the theoretic one of K_i equal infinite but 1.63 which is used in the simulation. This is because of the definition of the parameters K_i in Froude theory. As the first equation in the paper, K_i is the area ratio of air inlet divided by the rotor disk. In Froude theory, it is actually difficult to obtain the real value of the air inlet because the attachment point of the air on the shroud inlet, which might be more outside of the leading edge defined in the simulation, is hard to be clear. It could be changed with the environment and any dynamic factors. Therefore according to the comparison with simulation, here the real air inlet area in the Froude theory should be greater. Also for the theory, it does not consider the flow separation that has happened on the nozzle with greater radius as showed in the Fig.7. That is the reason why the shroud thrust keeps always increased and its difference between the theory for $K_i = \infty$ and the simulation becomes obviously after $R_e > 1.18R_r$.

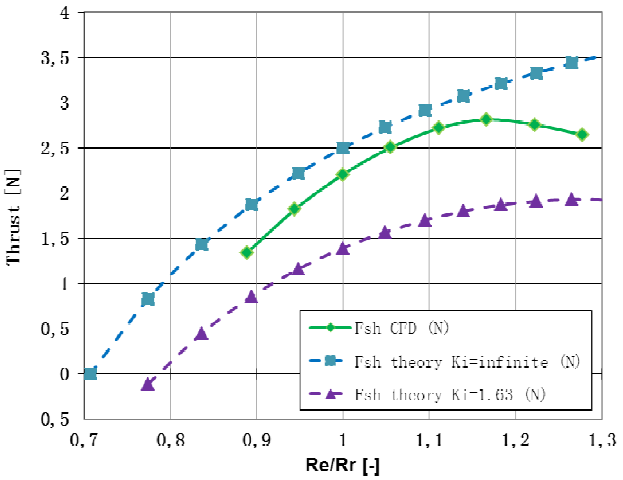

Fig. 8 Comparison with the CFD and Froude theory on shroud thrust F_{sh}versus R_e/R_r

More in depth, Fig.9 shows the power loading PL with varied radiusR_e from the Froude theoryespecially for $K_i = \infty$ and the simulation.

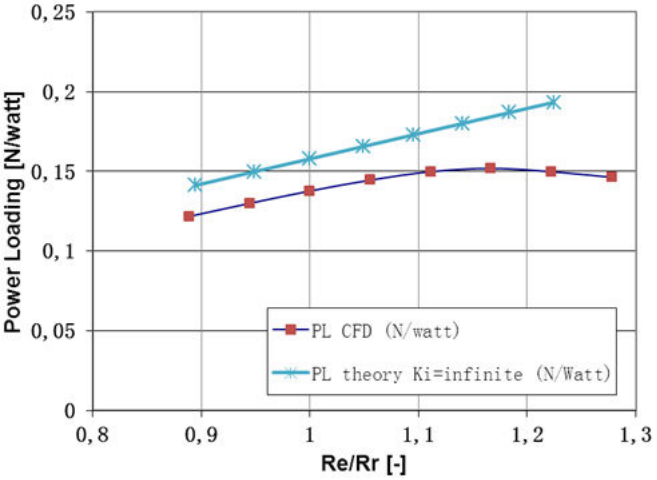

Fig. 9 PL&$\dot{m}$ versus R_e/R_r

Firstly, for the Froude theory combined the equations (2), (3), (10) and (11), the function of PL can be expressed:

$$PL = \frac{K_e}{\dot{m}} \cdot \left(2 - \frac{K_e}{K_i}\right) \cdot (\rho \cdot A_R) \tag{12}$$

For $K_i = \infty$and$F_T = 5\,\mathrm{N}$, by inducing (2) into the equation above, PL is:

$$PL = \sqrt{\frac{K_e \cdot (\rho \cdot A_R)}{F_T}} = \sqrt{\frac{(\rho \cdot A_R)}{F_T}} \cdot \frac{R_e}{R_r} \tag{13}$$

As showed in (13), under the condition of infinite inlet area, constant rotor radius and total thrust generation, PL from the Froude theory is the function only referring to the parameterK_e. Fig.9 properly shows a linear relation between PL and R_e/R_r .

Ithas globally similar trends of PL performance with the 2D simulation results:Generally more divergent nozzle improves the PL performance and behaves better as the analysis on the thrust performance. It implies that the more divergent nozzle has greater ability to perfectly expand the injected flow and converse the kinetic energy of the fluid into the pressure effect.

2) Internal nozzle shape

In reality itexists a lot of possibilities for the nozzle internal shape, the basic design rule is to adapt the flow structure as much as possible and avoid the flow separation to decrease the total pressure loss and drag as well. In this paper the internal nozzle shape was induced by the degree of convexity or concavity of the nozzle internal profile concerning to the external nozzle profile,this is showed as the subfigure of Fig.9. A set of eight cases were calculated. Case(a) means the internal shape is the most concave and case(h) is the one which is the mostconvex.

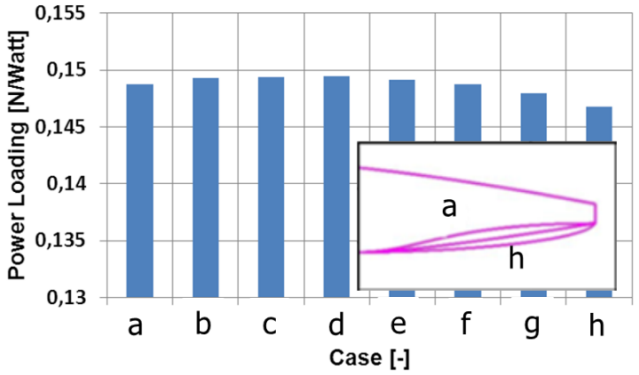

Fig. 10 PL versus cases with different internal nozzle shapes

Fig.10 indicates that a very low influence of internal nozzle shape on the global performance of power loading PL. The improvement on PL is limited by boundary layer separation due to the viscosity of fluid. Because of it, the variation of PL is reduced to about 1%.

The profile of shroud in 2D simulation is actually composed of four curvature lines P.1P.2, P.2P.3, P.3P.4 and P.4P.1 as showed in the subfigure in Fig.10. And another more important influence, that is the static pressure distribution along these four curvature lines, is showed in Fig.11. Comparing the extremely concave case(a) and extremely convex case(h), it is indicated that for the demand of total thrust 5 N,the pressure jumpsof both cases which could be seen on the point P.4 are almost the same, and they all result in a higher pressure gradient. It appears on the place where the nozzle profile (P.3 to P.4) has the greater curvature. And the comparison of the case(a) and (h) on PL reveals that the performance is extremely limited by the higher adverse pressure gradient on the nozzle exit P.3 as case h. This might lead to a relatively lower mass flow and then affect the region P.4P.1 of suction pressure which is weaker than the case (a).

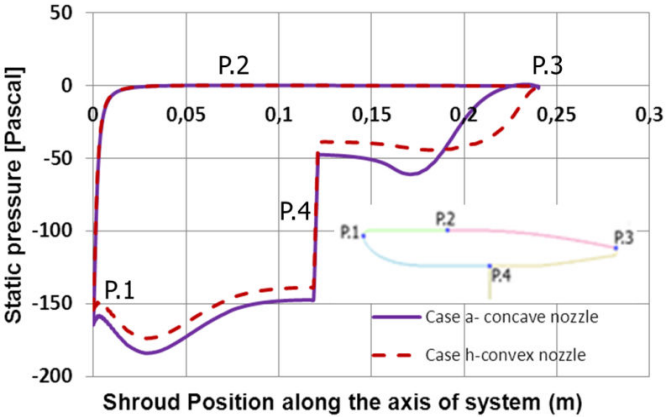

Fig. 11P_s on the shroud along system axis for case(a) and (h)

In conclusion, both extreme cases indicate that the curvature variation of nozzle internal shape should be smooth as much as possible, in order to avoid the higher adverse pressure gradient and keep from an early boundary layer separation.

3) Nozzle length and divergent angle

In the reality, it is not possible to change the nozzle length $l_N$independently. It is always related to the overall shape of the nozzle. Here in order to keep the overall shape constant, it is defined by the parameter divergent angle. It is obvious that the divergent angle θ is directly related to the nozzle length. Thus for each l_N, θ is varied from 7° to 17.5° with the step of 3.5°. Meanwhile for each divergent angle, the nozzle length is changed from 70 mm to 90 mm with the step of 10 mm as showed in the subfigure of Fig.12, this variation also correspondsto the change of nozzle radius.

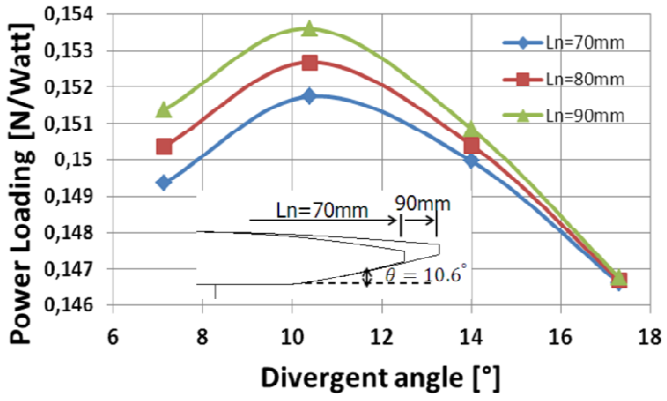

Fig. 12 PL versus l_n/R_r

Fig.12 shows the performance PL of three series of nozzle lengths with varied divergent angles. For all the nozzle lengths, the power loading is increased with increased divergent angle until $\theta = 10.5^\circ$, which is the optimal divergent angle to obtain the best PL performance, after that PL sharply drops down. It means at the divergent angle 10.5°,the profile of nozzle adapts the flow structure best. But it does not mean the nozzle could perfectly expand the mass flow. It is more dependent on the nozzle length. Fig.12 indicates that the longer the nozzle is, the

better the performance is. However, it is severely constraint by the greater nozzle radius along with the longer nozzle due to the flow separation happened on the nozzle exit. This is also the reason why the greatest divergent angle $\theta = 17.5^{\circ}$ drives the performances for all three series of nozzle lengths to the same value. For the nozzle with a relatively greater divergent angle, it naturally has greater risk to appear the boundary layer flow separation. And there is no sense to continue to increase the nozzle length because the effective nozzle radius will always keep the same and the increased nozzle length will not work at all for expanding the flow after rotors and also for the improvementof the system behaviors.

B. Influence of inlet design parameters

For the component inlet, it is a very important part to offer great part of the static thrust for shroud even for whole system. Its configuration is constrained by the parameters such as leading edge curvature, internal shape and length.

1) Leading edge curvature and internal inlet shape

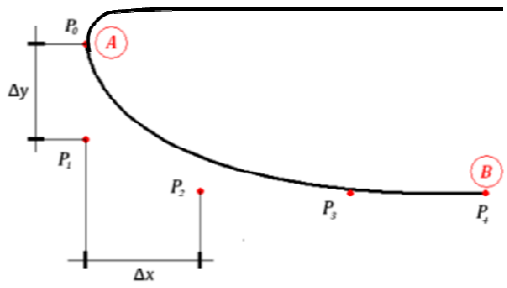

Fig. 13The B-spline of inlet lip

The curvature of a curve at one point is a measurement of how sensitive its tangent line is to moving the point to the nearby points. In this paper, the leading edge curvature C_{le} is referred to the one of points A in the Fig.13. According to the definition of curvature and by introducing the first and second order derivation of B-spline, Equation (14) was applied to calculate the leading edge curvature.

$$Curv = \frac{n-1}{n}\frac{\Delta x}{\Delta y^2} = \frac{3}{4}\frac{(x_2-x_1)}{(y_0-y_1)^2} \qquad (14)$$

Obviously, C_{le} at position A is controlled by the points P_0, P_1 and P_2. In this paper C_{le} is arranged from 0.045 mm^{-1} to 0.27 mm^{-1}, seen in the subfigure of Fig.13. Since the curvature is changed, the inlet internal shape might be changed along with it. In the reality, it is difficult to separate the geometry parameters which are originally related. Therefore particularly for internal shape, seven different ones with constant C_{le} = 0.15 mm^{-1}wereexplored.

In Fig.14, bothC_{le} and inlet internal shape have a minor influence on the PL. Based on the same C_{le} = 0.15 mm^{-1}, the variation with changed internal shape seems smaller than the one from the parameter C_{le} . Based on the simulations of these cases, the flow separation wasn't found, which might be happened on somewhere on the inlet. This implies, once the inlet could be designed to adapt the flow pattern and no boundary flow separation has happened, the effects on global performance by variation of geometry parameters can be ignored. The more important effects are on the pressure distribution.

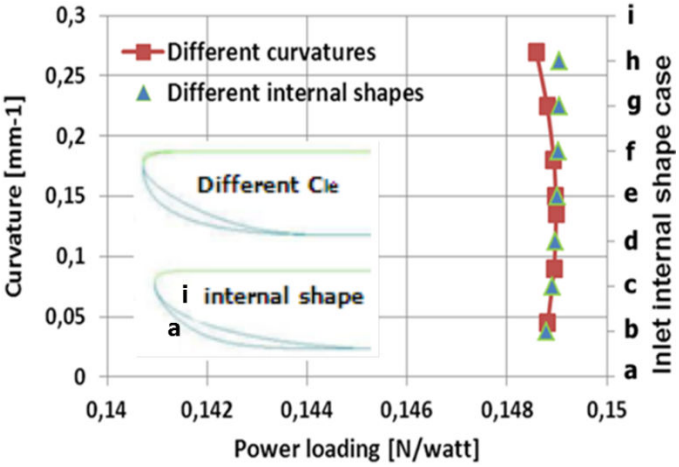

Fig. 14 PL versus C_{le} and inlet internal shape cases

Fig.15 shows a superposition of pressure distribution on shroud inlet along the radial axis for two different leading edge curvatures. For these two extreme cases of C_{le} = 0.045 and 0.27 mm^{-1}, they all could reach a suction peak at P.1, which is the reference position of leading edge curvature. A far lower pressure is formed at that position of C_{le} = 0.27 mm^{-1}. However it increasesdrastically until the second relative weaker suction peak appears on the place with lower curvature. For C_{le} = 0.045 mm^{-1}, globally the lower pressure keeps to be continuedand even much lower after the first suction peak even though there is a slightly recovery. It lets the shrouded system take full advantages of the curvatures along the inner inlet to produce more thrust.

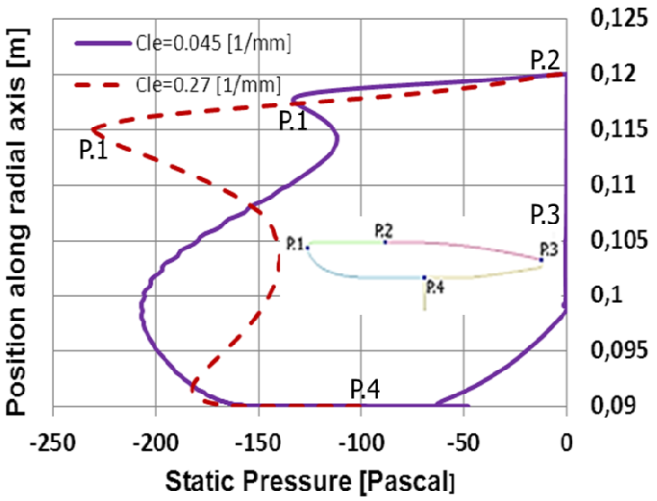

Fig. 15P_s on the shroud along radial axis for C_{le} = 0.045 and 0.27

The physical phenomenon could be revealed more clearly in the Fig.16. It shows that there is a continued lower pressure region formed on the inner inlet leading edge for $C_{le} = 0.045$. On the contrary, for $C_{le} = 0.27$ the suction peak is discontinued. It is separated by a relatively higher pressure, which is appeared after the beginning of inlet. It takes on a quite important region that can be used to generate more thrust. This is the reason why the PL performance tends to a decrement when the leading edge curvature is increased after one suitable value as showed in Fig.14.

As the exploration above, the system can benefit more if the pressure gradient is changed more smoothly or continuity. This greatly depends on whether the inlet design is adapted with the flow. That is critical to reduce the adverse pressure gradient to decrease the boundary separation risk.

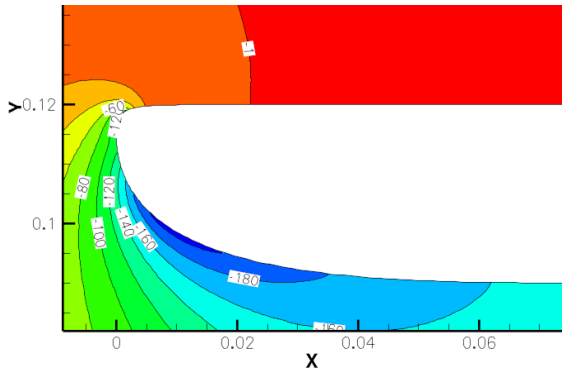

a) Static pressure distribution for $C_{le} = 0.045$

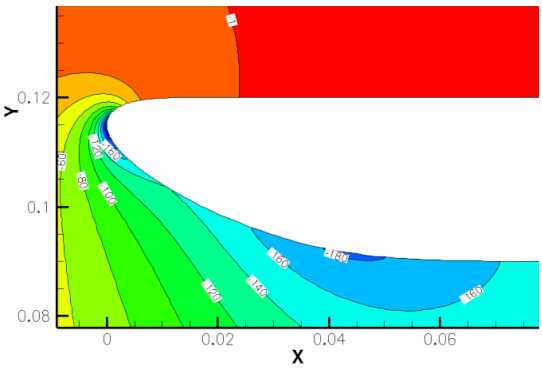

b) Static pressure distribution for $C_{le} = 0.27$

Fig. 16 Static pressure distribution for $C_{le} = 0.045$ and 0.27

2) Inlet length

The inlet length l_i was varied from 100 mm to 70mm with the step of 5 mm which corresponds to the ratio of l_i divided by the rotor radius, as seen in the Fig.17. It shows that l_i affects the global performance quite slightly. As the study above on the inlet leading edge curvature and internal shape, the more important is the effect on the pressure distribution. Except the consideration on loading other instruments, it is not worth to lengthen the inlet in views of the weight and size increment as same as nozzle length.

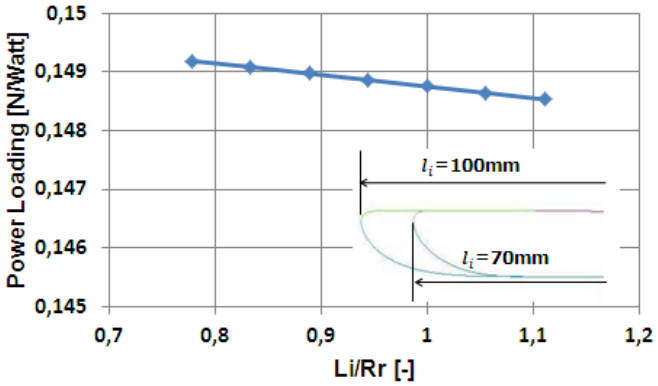

Fig. 17 PL versus$l_i/\mathrm{R_r}$

C. Influence of shroud maximum radius and leading edge radius

A combined study of two parameters: shroud maximum radius$\mathrm{R_{max}}$ and leading edge radius R_{le}, was made. $\mathrm{R_{max}}$was changed from 110 mm to 170 mm with the main step of 5mm which corresponds to the ratio of$\mathrm{R_{max}}$ divided by the rotor radius 90 mm from 1.22 to 1.89. The increment of $\mathrm{R_{max}}$ means an increment of shroud thickness. For each $\mathrm{R_{max}}$, two or three different values of R_{le} from $R_{le} = (\mathrm{R_{max}} - 15)$mmto $R_{le} = (\mathrm{R_{max}} - 5)$mm were studied. One example of the geometry was showed in Fig.18.

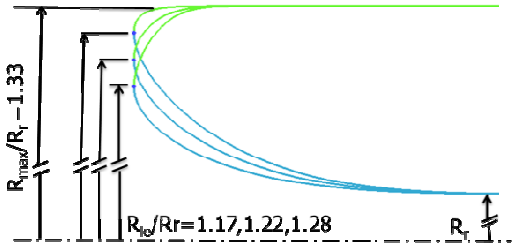

Fig. 18 Geometry scheme for $\mathrm{R_{max}}/R_r = 1.33$ and$\mathrm{R_{le}}/\mathrm{R_r} = 1.17, 1.22, 1.28$

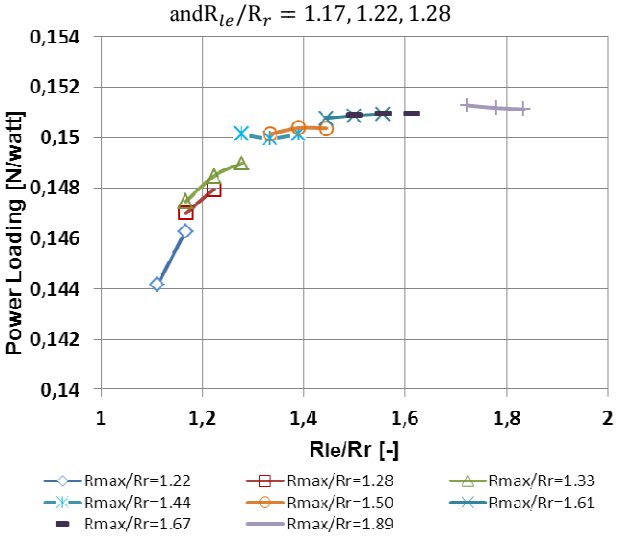

Fig. 19 PL versus $\mathrm{R_{le}}/\mathrm{R_r}$ for different $\mathrm{R_{max}}$

Fig.19 shows the power loading performance of all systems with different leading edge radius and maximum radius. Asignificant improvement of the performance on PL could be found as the increment of both R_{max} and R_{le} until the stabilization occurs, that is $R_{max}/R_r > 1.5 or R_{max} > 135mm$. Under this condition,the overlapping points on PL of 0.1465 N/Watt with different values of $R_{max}/R_r = 1.22$, 1.28 and 1.33 can reveal the less importance of the parameterR_{max} on PL before the stabilization appearance. Compared to it, the parameter R_{le} playscritical role on improving the system behaviors. PL is increased along with the increment of leading edge radius.

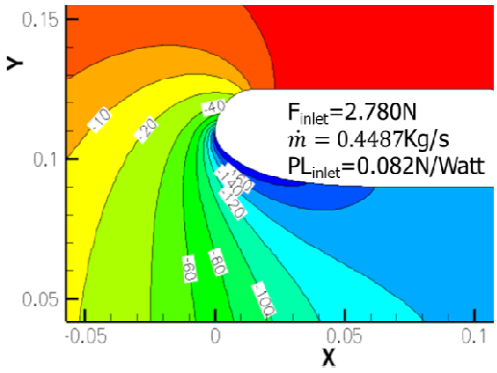

a. $R_{le}/R_r = 1.17$

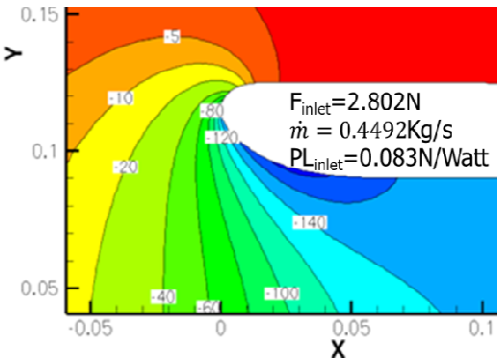

b. $R_{le}/R_r = 1.22$

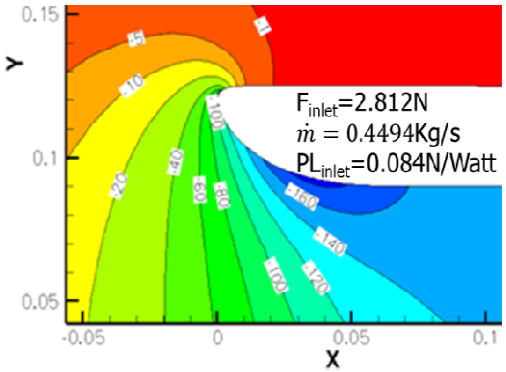

c. $R_{le}/R_r = 1.28$

Fig. 20 Static pressure distribution on inlet for $R_{max}/R_r = 1.33$ and$R_{le}/R_r = 1.17, 1.22, 1.28$

Fig.20 reveals that the variation of R_{le}/R_r from 1.17 to 1.28 makes a backward movement of the suction peak formed on the inlet. Although the most important lower pressure region is nearby the leading edge, this movement can still increase the suction region. And also the greater leading edge radius gives more possibility to widen the lower pressure internal surface. The shroud inlet with relative largest leading edge radius $R_{le}/R_r = 1.28$ can therefore aspirate more mass flow $\dot{m} = 0.449$ Kg/s and then produce the greatest thrust 2.812 N. This increased thrust from inlet contributes most on the power loading improvement of the whole systems such as PL of 0.084 N/Watt produced by the inlet with $R_{le}/R_r = 1.28$.

However, this importance becomes less when the $R_{max}/R_r > 1.5$in Fig.19. The performance PL keeps almost constant with varied both $R_{le}$and R_{max} . Considering the additional size and weight along with increased R_{max} , the benefit of PL performance from it should be balanced with these disadvantages.

V. Conclusion

This paper conducted a parametrical study of the shroud with the rotor modeled as an actuator disk of radius 90mm. Based on the extraction of the shroud geometry parameters, it has revealed the effects of each parameter on the system performance, and explored which of the different parameters considered would be relevant for the optimization of the power loading. The main conclusion could be obtained as following:

For the nozzle, the power loading is improved greatly with a greater nozzle radius. However it is limited by the appearance of boundary layer separation, this actually decreases the effective nozzle radius and produces a pressure loss. The internal shape might be an important factor, but in reality its effect is drastically reduced due to the viscosity. Lengthening the nozzle length can improve the system, but it is constrained by the nozzle divergent angle. The optimal designed divergent angle for different nozzle length is kept to around 10.5°;

For the inlet, once the inlet is designed to adapt the flow structure, the improvement by changing any inlet parameters will be limited. The shroud maximum radius and leading edge radius are relevant. The variation of maximum radius must change the leading edge radius to some degree due to the geometry integration. The incensement of both parameters means an incensement of inlet internal surface, that is could aspirate more air and widen the low pressure region and finally improve the system. But it is limited by greater maximum radius;

The other parameters have a low influence which will not make the difference on the power loading greater than 1%. However, they play an important role in pressure distribution along the shroud. The basic design criterion is to reduce the risk of boundary layer separation both on the inlet and nozzle.

Acknowledgment

The author is grateful for the support and facilities from the department of aerodynamic, energetic and propulsion of InstitutSupérieur de l'Aéronautiqueet de l'Espace.

REFERENCES

[1] Black, D., "Shrouded Propellers- A Comprehensive Performance Study", *AIAA 68-994*, Oct.1968;
[2] Kruger, W., "On Wind Tunnel Tests and Computations Concerning the Problem of Shrouded Propellers", *NACA TM No.1202*, Feb.1949;
[3] Cycon, J., "Sikorsky Aircraft UAV Program",*Vertiite*, V.38, No.3, May. 1992;
[4] Lipera, L., "The Micro Craft iSTAR Micro Air Vehicle: Control System Design and Testing", *AHS57th Annual Forum*, May 2001;
[5] Kailash, K., "Ducted Fan or Shrouded Rotor Aerodynamics and its Applications in VTOLMiniature Aerial Vehicles", *AE 416 project*,Dec.2005;
[6] Tayor, R., "Experimental Investigation of the Effects of some Shroud Design Variables onthe Static Thrust Characteristics of a Small Scale Shrouded Propeller Submerged in a Wing",*NACA*, Jan.1958;
[7] Jason Pereira, et al, "Performance and Surface Pressure Measurements on A MAV-ScaleShrouded Rotor in translational flight", *American helicopter Society International*, May 1-3, 2007;
[8] Fleming, J., "Improving Control System Effectiveness for Ducted Fan VTOL UAVs Operating inCrosswinds", *AIAA Paper*, 2003-6514;
[9] Dyer,K., "Aerodynamic Study of a Small, Ducted VTOL Aerial Vehicle", *M.S Thesis, MassachusettsInsitute of Technology*, Jun.2002;
[10] Hui When Zhao, and CeesBil, "Aerodynamic Design and Analysis of a VTOL Ducted-FanUAV", *26th AIAA Applied Aerodynamics Conference*, August 18-21, 2008;
[11] Andy Ko., "Ducted Fan UAV Modeling and Simulation in Preliminary Design", *AIAA Modeling and Simulation Technologies Conference and Exhibit*, Aug 20-23,2007;
[12] Hui, W. Z., Bil, C. and Bok, H. Y., "Computational Fluid Dynamics Calculations on Preproduction Ducted Fan VTOL UAV for Stability andControl",*3rd Australasian Unmanned Air Vehicles Conference*, 9 - 12 March, 2009.